Photoionization of singly and doubly charged aluminum ions in the extreme ultraviolet region: Absolute cross sections and resonance structures

J. B. West
CLRC Daresbury Laboratory, Warrington WA4 4AD, United Kingdom

T. Andersen, R. L. Brooks,* F. Folkmann, H. Kjeldsen, and H. Knudsen
Institute of Physics and Astronomy, University of Aarhus, DK-8000 Aarhus C, Denmark

(Received 7 November 2000; published 19 April 2001)

Absolute measurements of the photoionization cross sections of Al^+ ions ranging from 20 to 160 eV and of Al^{2+} ions from 70 to 105 eV have been performed utilizing a merged-photon–ion-beam setup with synchrotron radiation from an undulator. The continuum cross sections are in good agreement with published theoretical predictions. Structures resulting from excitation of valence or inner-shell electrons are resolved, identified, and compared with assignments from earlier spectral measurements. The analysis of the spectra is performed with the support of multiconfigurational atomic structure calculations.

DOI: 10.1103/PhysRevA.63.052719 PACS number(s): 32.80.Fb, 32.80.Dz

I. INTRODUCTION

The development of computational methods for the prediction of atomic properties, such as oscillator strengths for inner-shell photoexcitation or absolute cross sections for inner-shell photoionization, has created a strong need for experimental data to test the predictions and to guide future theoretical developments. Absolute photoionization cross sections in particular are required for an in-depth understanding of many laboratory plasma and astrophysical phenomena. It is also possible to understand features in atomic spectra from a knowledge of the intensities of autoionizing transitions in the experimental spectra, by calculating the oscillator strengths of the transitions from the absolute cross section data. The requirement for data of this kind is evident from the fact that several large theoretical programs have been devoted to the task, in particular the Opacity [1], OPAL [2], and IRON [3] projects as well as a large number of predictions published in individual articles.

The ongoing development of synchrotron radiation (SR) facilities, leading to much improved photon flux from insertion devices such as undulators, has now made it possible to perform detailed tests of theoretical predictions. Experimental facilities aimed at measuring absolute photoionization-cross-sections for singly and multiply ionized ions have been developed at Berkeley (ALS), Paris (LURE), Tsukuba (Photon Factory), and Aarhus (ASTRID). Absolute photoionization cross-section data were first reported more than a decade ago [4] from the Daresbury Laboratory by Lyon *et al.* utilizing photons from a bending magnet, but the limited photon flux made it possible to study only ions exhibiting large cross sections (Ca^+, Sr^+, Ba^+, K^+, Zn^+, Ga^+), in contrast to many of the ions of astrophysical importance (for example, C^+, N^+, O^+, and Mg^+). Improvements in SR light sources since that time have made it possible to make measurements of ions of astrophysical interest, most recently C^+ [5] and Mg^+ [6], where the latter has a cross section of only 0.2 Mb close to the threshold region. These studies have also been able to yield more information about the structure associated with autoionizing transitions, and have led to alternative identifications, as was the case with the $2p \rightarrow ns$ and $2p \rightarrow nd$ excitations in Mg^+. For some time it has been known that configuration interaction influences the strengths and positions of the transitions observed in Mg^+, but it became clear from determinations of the oscillator strengths that this interaction may have been overestimated in earlier calculations performed to account for the original experimental data obtained by Esteva and Mehlman [7] from vapor plasma discharge measurements.

In contrast, the situation for the corresponding transitions in the photoionization of the Al^+ ion may be more complex. Costello *et al.* [8] performed *ab initio* atomic structure calculations in order to analyze their dual-laser plasma measurements carried out in the same spectral region as that of this paper, and were able to identify most of the structure seen. Contributions from photoexcitation of the metastable $3s3p\ ^3P\,Al^+$ ion have also been identified [9]. Of particular interest was the prominence of doubly excited states involving the $3p^2$ configuration, and the strong interaction of these with the single-electron transitions.

In the present experiment we are able to provide reliable values both for the absolute continuum photoionization cross sections, making tests of theoretical predictions possible, and to provide new information about the resonance structures including the relative intensities of the lines by calculating their oscillator strengths from the absolute cross sections. In this way we can provide new or additional information on their identity. The $^1S_0$ ground state of the Al^+ ion has the configuration $2p^6 3s^2$, with an admixture of the $2p^6 3p^2$ configuration [10]. The production of pure Al^+ ground-state beams is difficult due to the existence of the long-lived metastable $2p^6 3s3p\ ^3P$ state, leading to a minor contamination of the ground-state beam. The extent of this contamination can, however, be established so that absolute measurements can still be obtained.

*Permanent address: Guelph-Waterloo Physics Institute, University of Guelph, Guelph, Ontario, Canada N1G 2W1.

In addition, we have been able to carry out similar measurements on the Al^{2+} ion. Direct comparisons can therefore be made with the isoelectronic Mg^{+} ion, with the advantage that the Al^{2+} spectra are spread over a wider energy range. This simplifies identification of the structure, given the resolution limitations of our experiment. Related studies of the doubly charged aluminum ions have been performed by Brilly *et al.* [11], who investigated the photoabsorbtion spectrum of Al^{2+} using the duo-laser plasma technique, with emphasis on excitation of the $2p$ electrons, and by Thomason and Peart [12] who studied electron-impact ionization of Al^{2+}, a topic that has attracted significant theoretical interest, see Teng [13] and references therein.

It should be noted that a recent introduction to the field of vacuum ultraviolet photoionization of atoms, ions, and molecules is available [14], and that the wide use of electron spectroscopy in connection with synchrotron studies of atoms has been covered by Schmidt [15].

II. EXPERIMENT

The experiments were carried out using a merged-beam layout very similar to that used by Lyon *et al.* [4]. A full description of the experimental layout has been given by Kjeldsen *et al.* [16]. In summary, the interaction between ions and photons was obtained by merging a 2–4 keV beam of Al^{+} or Al^{2+} ions with a synchrotron-radiation beam over a distance of 50 cm. The single- and double-photoionization cross sections were determined from the photoionization yield of ions having lost one or two electrons. The experiment was set up on an undulator beam line at the 580-MeV storage ring ASTRID at the University of Aarhus. Photon fluxes of typically $\sim 10^{12}$ photons/sec 0.1% bandwidth were obtained and detected by a calibrated Al_2O_3 photodiode. The photon-energy resolution varied between 60 meV and 1.0 eV in the experiments described here, but spectra at higher resolution were also taken in the fourth order and assisted in identifying much of the weaker structure not resolved in the first-order spectrum. As in the previous work, the photon-energy calibration (which includes a small Doppler shift) is expected to be correct within ± 20 meV and was performed using autoionizing resonances in He (at ~ 60 eV) and Kr (~ 90 eV), observed in a noble-gas ionization chamber. The required resonance energies were obtained from the literature [17,18].

The Al^{+} and Al^{2+} ions, respectively, were produced in their ground state in a Nielsen-type ion source [19], accelerated to 2 or 4 keV and then deflected by an electromagnet that allowed only the ions of interest to pass. The calibration procedures and beam profile measurements were carried out as described previously [16]. The expression

$$\sigma = S \frac{e^2 \eta v F(\Delta x)(\Delta y)}{IJ\Omega \ell} \tag{1}$$

was used to calculate the single-photoionization (or double-photoionization) cross section from the experimental measurements. S was the recorded count rate of doubly or triply charged ions produced in photoionization, e the electronic charge, F the form factor that is a measure of the overlap between the photon beam and beam of singly charged ion, Δx and Δy the sampling intervals in the measurements of the beam profiles, I the current of target ions measured by the Faraday cup (for doubly charged target ions I was replaced with $I/2$), J the photodiode current, η the photodiode efficiency, Ω the efficiency of the Johnston multiplier for detecting photoionized ions with the concerned energy and charged and ℓ the interaction path length.

In the case of the Al^{+} beam, a minor contamination of the ground-state beam was observed from the spectra recorded in the 70–72 eV region, representing the excitation of the metastable $2p^6 3s 3p\ ^3P$ ion to the $2p^5 3s^2 3p\ ^3S$, P, or D states. On the basis of intensity measurements of the $2p^6 3s 3p\ ^3P_2 - 2p^5 3s^2 3p\ ^3D_3$ line, representing the metastable component, and of the $2p^6 3s^2\ ^1S_0 - 2p^5 3s^2 4s\ ^1P_1$ line, representing the ground-state component, and utilizing the calculated oscillator strengths for these two transitions [9], it was possible to determine the content of the metastable component in the ground-state beam to be 5%. It was possible by lowering the anode voltage to reduce the content of the metastable component to 3%, but the intensity of the ground-state beam was thereby also reduced to a level making the measurements difficult and time consuming.

The accuracy of the absolute cross sections is estimated to be 10–15 %.

III. CALCULATIONS

We have used the multiconfiguration Hartree-Fock (MCHF) method [20] in a manner described before, see Ref. [21]. We have used a level of configuration interaction sufficient to allow us to assign spectral lines with some confidence. Specifically, the three electrons in orbitals higher than $n=2$ were permitted to make all $3s$, $3p$, $3d$, and $4s$ substitutions, as well as $2p^6$, consistent with LS coupling and parity constraints. The program GENCL [22] was used to generate a list of interacting configurations that typically numbered between 20 and 40. The energy level was assigned based on the largest mixing coefficient. All orbitals were allowed to vary, and the program's default parameters were used throughout.

For a configuration with three open shells, such as $2p^5 3s^3 p^2$, many terms are possible and we have limited our examination to terms excited from the ground-state configuration that can yield $J=1$; i.e., ^3S, ^1P, ^3P, and ^3D. Parentage considerations yield two ^3S, three ^1P, four ^3P, and three ^3D terms. In the cases where excitation of the metastable component is investigated a larger set of terms has been considered, taking terms with $J=1$, 2 or 3 into consideration.

For the Mg^{+} and Al^{2+} assignments, a configuration interaction (CI) calculation was performed because the levels of interest lie close together and strongly interact. The $2p^5$ electrons were coupled last to the outer electrons to try to simulate realistic coupling. The outer electrons were configured as $3p^2$, $3s3d$, $3s4s$, $3s4d$, and $3s5s$ and all coupling combinations leading to $^{2,4}S$, $^{2,4}P$, and $^{2,4}D$ were included for a total of 27 such configurations. However, there is a program-

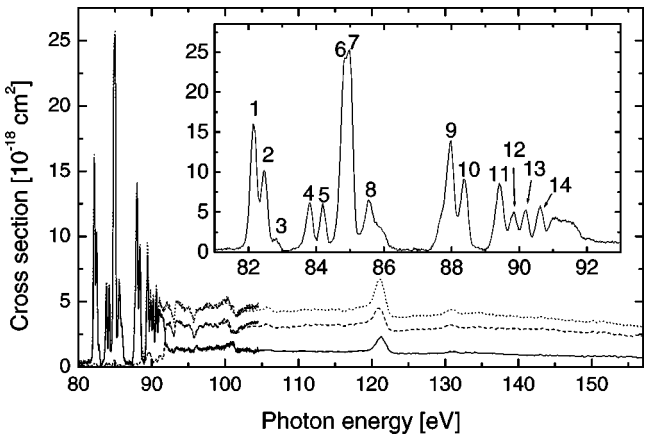

FIG. 1. The partial Al^+ photoionization cross sections for production of Al^{2+} (full line) and Al^{3+} (dashed line) and the sum of these two cross sections (dotted line), which is the total photoionization cross section in the photon energy region 80–160 eV. The features numbered are listed in Table I.

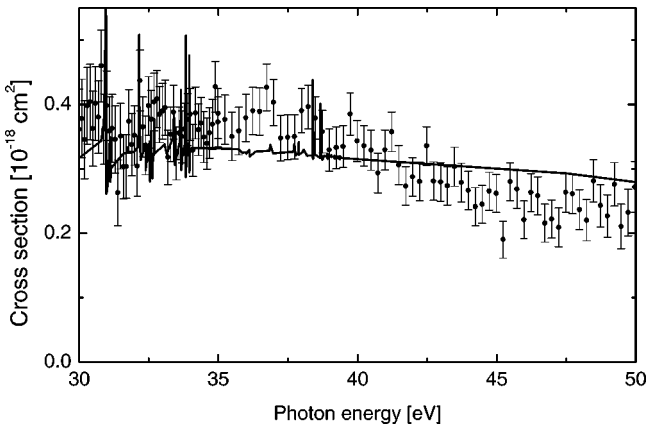

FIG. 2. The (single-) photoionization cross section for Al^+ in the photon-energy range 30–50 eV. The experimental data (solid circles and statistical error bars) were recorded with a Mg-foil inserted in the photon beam to eliminate higher-order radiation; the theoretical data (full line) are from the Opacity project [25].

ing dimensional limitation of 20 configurations so the calculation was performed in steps dropping the least interacting configurations when adding additional ones and checking for self-consistency throughout. The programs utilized from the atomic-structure package of Froese Fischer *et al.* [20] were GENCL, BREIT, CI, MLTPOL, and LSJTR.

IV. RESULTS AND DISCUSSION

A. Al^+

The continuum photoionization cross section of ground-state Al^+ ions can be divided into the following energy regions.

(a) The region above 91.71 eV, representing the photoionization of a $2p$ electron and at some higher energies of a $2s$ electron. Since the cross section for photoionization of an inner electron is hardly influenced by the valence electrons, the admixture of metastable ions can be neglected.

(b) From threshold for production of Al^{2+} ions at 18.83 eV, representing photoionization of a $3s$ electron, to the threshold for photoionization of a $2p$ electron. In this energy region the cross section is dependent on the valence electrons. The admixture of metastable ions will lead to the cross section being too large if a correction is not made.

In Fig. 1 we show the total continuum cross section together with the cross sections for single and double ionization in the energy region above the $2p$ threshold. The continuum cross section reaches a maximum value near 100 eV at a value of 5.0(5) Mb and slowly decreases to 3.3(4) Mb near 160 eV. The main contribution comes from the double ionization channel. Superimposed on the smooth continuum cross section, resonance structures can be seen in this channel below 105 eV, and in both channels around 122 eV and 132 eV. These structures will be discussed below.

Theoretical predictions of the $2p$ photoionization cross section have been available for quite some time and they are generally in good agreement with, but slightly larger than the present experimental observations. Combet Farnoux and Lamoureux [23] predicted a maximum cross section of 6.0 Mb at 100 eV, using the central-potential model followed by a decrease to 3.5 Mb at 160 eV, whereas Deshmukh *et al.* [24] obtained a slightly lower maximum (5.5 Mb) from a relativistic random-phase approximation calculation, but a similar cross section near 160 eV. The latter calculation also indicated a small increase in the cross section with the onset of the $2s$ threshold near 137 eV, but the change is too small to be observed in the experimental data.

The continuum cross section in the region from the threshold for production of Al^{2+} ions to the photoionization of a $2p$ electron is much smaller than the cross section discussed above. Figure 2 shows the photon region 30–50 eV. The absolute photoionization cross section in this energy region will consist not only of a contribution from photoionizing a $3s$ electron from the ground state or from the metastable beam, but also of a contribution from photoionizing a $3p$ electron in the metastable component. The ratio between the cross sections for photoionizing the Al^+ ion having a $3s3p$ compared to a $3s^2$ valence shell is very close to 1.25, according to calculations performed within the OPACITY project in the 30–50 eV region. We have used this ratio to establish the absolute cross section for the Al^+ ground-state ion, taking into consideration that our beam contains 5% of the metastable level $3s3p^3P$. Thus the maximum cross section for $3s$ photoionization, which appears around 32 eV, will have a value of 0.38 Mb, decreasing to approximately 0.24 Mb at 50 eV. This is in relative good agreement with the values predicted from the OPACITY project [25], from which a cross section ranging from 0.34 Mb to 0.28 Mb was reported for this energy region.

The resonance structures appearing in Fig. 1 are due to excitation of a $2p$ or a $2s$ electron. Since the ground state of Al^+ is best described by the $2p^63s^2$ configuration with a contribution from $2p^63p^2$ and there also is a minor admixture of metastable $2p^63s3p\ ^3P$ ions in the primary beam we have to consider excitations of all three configurations to explain the observed structures. The dominant structures appear in the single-ionization channel between 82 and 92 eV

TABLE I. The energies, oscillator strengths (f values), and assignments for the spectral features of Al^+ numbered in Fig. 1. The f values were obtained assuming 100% population of the ground state in the target beam.

Line No.	Energy (eV)	Energy [a] (eV)	Assignment [a]	Oscillator strength	n^*
1	82.15	82.15	$2p^5 3s[3p^2(^1D)]\ ^3D_1$	0.035	2.38[b]
2	82.47	82.45	$2p^5 3s[3p^2(^1D)]\ ^1P_1$	0.022	2.36
3	82.81	82.77	$2p^5 3s(^1P)3p^2(^3P)\ ^3P_1\ rev$	0.028	2.47[b]
4	83.79	83.77	$4s(^1P)_1$	0.014	2.62[b]
5	84.19	84.17	$4s(^3P)_1$	0.012	2.61
5a	84.44	84.50	$2p^5 3s[3p^2(^1S)]\ ^3P_1$	0.002	2.75[b]
6	84.79	84.78	$2p^5 3s[3p^2(^1S)]\ ^1P_1$	0.042	2.72
7	84.99	84.99	$3d(^1P)_1 rev$	0.051	2.83
7a	85.36	85.26	$3d(^3D)_1 rev$	0.005	2.81
8	85.57	85.56	$3d(^3P)_1 rev$	0.014	2.86[b]
8a	87.68	87.65	$5s[3/2,1/2]^1P$	0.010	3.69[b]
9	87.96	87.93	$4d[3/2,5/2]^1P$	0.034	3.83[b]
10	88.37	88.31	$4d[1/2,3/2]^3D$	0.023	3.80
11	89.41	89.33	$5d[3/2,5/2]^1P$	0.025	4.86[b]
12	89.81	89.73	$5d[1/2,3/2]^3D$	0.015	4.88
13	90.18	90.10	$6d[3/2,5/2]^1P$	0.013	5.98[b]
14	90.61	90.52	$6d[1/2,3/2]^3D$	0.012	6.02

[a]From Ref. [8] and the present calculations.
[b]Calculated using the $^2P_{3/2}$ ionization limit.

and in the double-ionization channel below and above the threshold for $2p$ ionization. Far above the $2p$ photoionization threshold Fano-type resonances can be seen around 122 eV and 132 eV.

The rather intense structures between 82 and 92 eV are due to $2p \rightarrow nd$ transitions, with n being 3 or larger, followed by weaker structures of $2p \rightarrow ns$ with n being 4 and 5, but it is not surprising that configurations including the $3p^2$ structure also are populated to a significant extent. Calculations showed that the dominant line 7 should be assigned to the $2p^6 3s^2\ ^1S_0 \rightarrow 2p^5 3s^2 3d\ ^1P_1$ transition, with line 8 representing $^1S_0 \rightarrow {}^3P_1$. These assignments differ, however, from the previous assignments [8], since line 7 in that work was attributed to the $^1S_0 \rightarrow {}^3P_1$ transition. However, the intensities of the two lines are inconsistent with the previous identification. The higher members of the $2p \rightarrow nd$ Rydberg series can be identified, in good agreement with our calculations. Due to the strong spin-orbit coupling for the excited states it can also be expected that singlet→triplet transitions may be rather intense (peaks 10, 12, and 14), which is in good agreement with our calculations. Only the total angular momentum J is a good quantum number for the excited triplet states that may either have a ^3D or ^3P term as the leading eigenvector.

The $2p \rightarrow ns$ transitions are weaker than the $2p \rightarrow nd$ transitions, as also noticed for the similar transitions in the Mg^+ ion [6], but in Al^+ these transitions are better separated from the nd series, so peaks 4 and 5 can be assigned unambiguously to transitions to the $2p^5 3s^2 4s\ ^1P_1$ and $^3P_1$ states. Due to the multiexcitation processes taking place during excitation of an inner electron and since the ground-state configuration of the Al^+ ion contains a contribution from $3p^2$, it is to be expected that excited states containing the $3p^2$ structure will be strongly populated. From our calculations we see that this is particularly noticeable for line 6, the transition to the $2p^5 3s(^1P)3p^2(^1S_0)^1P_1$ state; our assignments for lines 1–3 show that other $3p^2$ terms also are involved as a result of multielectron excitation.

Table I lists the prominent lines from Fig. 1 in the energy region from 82 eV to 92 eV. Given the limited resolution of our experiment, not all calculated lines are shown since they could not be observed; in the higher resolution experiments of Costello *et al.* [8] for Al^+ and Brilly *et al.* [11] for Al^{2+} additional lines are identified. The energies, oscillator strengths, and assignments are given together with the effective quantum numbers, which are calculated on the basis that all the lines we observe converge to the $^2P_{1/2,3/2}$ limits. These limits were taken from Ref. [8], where they were calculated from known values of the ionization potential of Al^+ and the transition energies $2p^6 3s(^2S_{1/2}) \rightarrow 2p^5 3s(^2P_{1/2,3/2})$. The assignments given in Table I have also been taken from Ref. [8] and confirmed or modified by our own calculations, the latter being marked *rev* in the table. The first revision is the assignment of the $2p^5 3s(^1P)3p^2(^3P)^3P$ term to the line at 82.77 eV. Our calculations show this term to be 2.4 eV lower than the $2p^5 3s(^3P)3p^2(^3P)\ ^3P$ term that would produce a likely blend with $2p^5 3s^2 3d\ ^3D$. The second is that we assign the transition at 85.26 eV to the $2p^5 3s^2 3d\ ^3D$ term. This replaces the $2p^5 3s(^3P)3p^2(^3P)\ ^3D$ assignment of Ref. [8], since this transition would have a lower-state counterpart of $2p^5 3s(^1P)3p^2(^3P)\ ^3D$ that we calculate to be a full 5-eV lower in energy. There are no lines at this energy in the spectrum, and since these two states are strongly mixed it is hard to see why one would contribute to

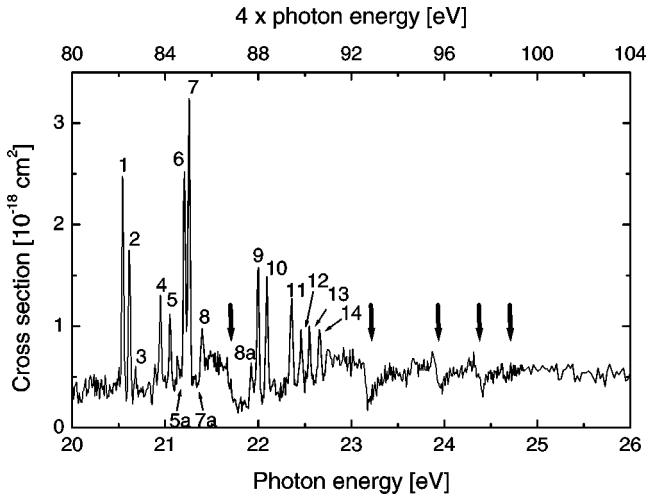

FIG. 3. The apparent single-photoionization cross section for Al^+ from 20–26 eV. Contrary to the data shown in the other figures the data shown in this figure are significantly influenced by higher-order radiation. The fourth-order spectrum for the yield of Al^{2+} (the numbered features that are also listed in Table I) is prominent, covering the same range as in Fig. 1 but with enhanced resolution; the top axis shows the photon energy multiplied by 4 in order to facilitate comparison with Fig. 1. The structure in the first-order spectrum is marked by arrows; see Table II.

the spectrum while the other would not. The assignments of lines 7 and 8 have also been revised for the same reasons.

The optical configuration of the grazing incidence monochromator used for this work was selected to enhance its order-sorting properties, but it has been known for some time that the selective-reflection principle on which it relies is not effective at low photon energies [26]. We have been able to take advantage of this, fortuitously, in the case of our measurements of Al^+ by observing the fourth-order spectrum, where the resolution is enhanced. This was possible in spite of the fact that the fraction of fourth-order radiation was small ($\sim$1.3% of the total flux) because the peak cross sections due to excitation of the $2p$ electrons are much larger than the continuum cross section in the threshold region. The results are shown in Fig. 3, and we have used this spectrum to identify additional lines 5a, 7a, and 8a, also listed with their effective quantum numbers in Table I and the assignments of the nearest lines from Ref. [8]. Furthermore, by using these data it was possible to give more reliable values of the oscillator strengths of transitions that were hardly resolved in the first-order spectrum. The first-order spectrum, free from higher-order radiation, was used to provide the oscillator strength of a group of partly resolved lines, and the fourth-order spectrum then used to separate the contributions of the individual lines. Also shown in Fig. 3 are members of the $3pns$ series, seen in first order and appearing as window resonances. They are in excellent agreement with our MCHF calculations and with the predictions of Butler *et al.* [25] (see Table II).

The presence of metastable ions in the ion beam is clearly evident from the resonance structures observed with 70–72-eV photons. These structures are shown in Fig. 4 with the prominent structures identified as due to the $2p \rightarrow 3s$ excitation of the metastable ions [9]. It should be noticed that no structures with $J=0$ are observed, confirming that the excitation involves only the metastable $^3P_2$, and $^3P_0$ components, whereas the $J=1$ component, which is mixed with the short-lived $^1P_1$ component, will decay to the ground state during the flight time from the ion-source to the interaction region. In contrast, spectra obtained from a laser-produced plasma [9] contain resonance lines originating from excitation of the two short-lived $J=1$ levels, illustrating that the excitation takes place within a few nanoseconds after production of the ions.

TABLE II. Members of the $3pns$ series shown in Fig. 3.

Energy (expt.) (eV)	Energy (theory)(eV) [25]	Energy (theory) (eV)	Identity
21.71	21.84	21.76	$2s^2 2p^6 3p5s\ ^3P$
23.18	23.22	23.21	$2s^2 2p^6 3p6s\ ^3P$
23.94	23.94	23.97	$2s^2 2p^6 3p7s\ ^3P$
24.40	24.38	24.42	$2s^2 2p^6 3p8s\ ^3P$
24.67	24.66	24.71	$2s^2 2p^6 3p9s\ ^3P$
		25.48	$2s^2 2p^6 3p^2 P$-limit

The resonance structures seen between 82 eV and 88 eV in the double-ionization channel (see Figs. 1 and 5) are identical to, but much weaker than, the resonance structures present in the single-ionization channel. Since the photon energy available is sufficient to remove two electrons from the target ions, the identity of the spectra indicates that the resonance structures originate from the same excited states. However, above 88 eV there is a significant difference between the two channels. Whereas the structures appearing in the single-ionization channel can be accounted for by excitation of the ground-state ions (see Table I), the origin of the much weaker resonance structures in the double-ionization channel may be different.

The evidence of further structure in the spectrum results from the comparison between the Al^{2+} and Al^{3+} spectra shown in Fig. 5 in the region between 88 and 92 eV, which

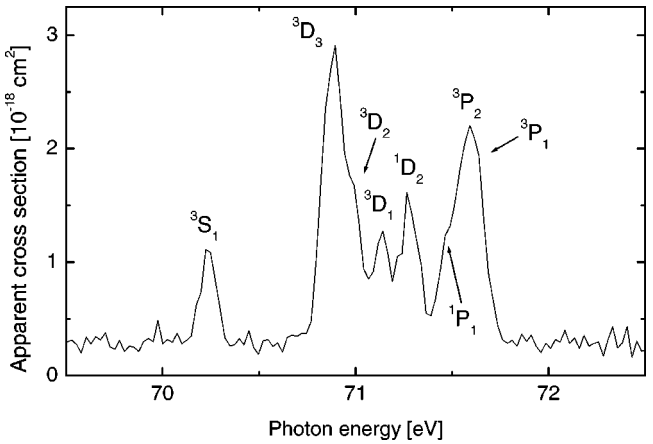

FIG. 4. The apparent photoionization cross section of the $3s3p$ metastable level of Al^+; the assignments follow those given in Costello *et al.* [8].

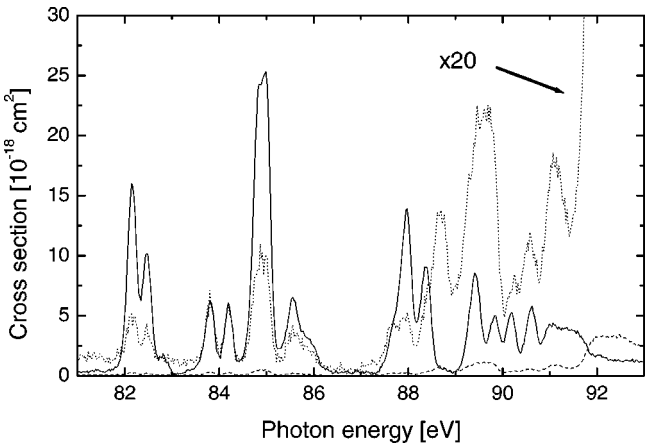

FIG. 5. Comparison of the measured single- (full line) and double-photoionization (dashed line) cross sections of Al^+ in the photon-energy range 81–93 eV. Also shown is the double-photoionization cross section multiplied by 20 (dotted line).

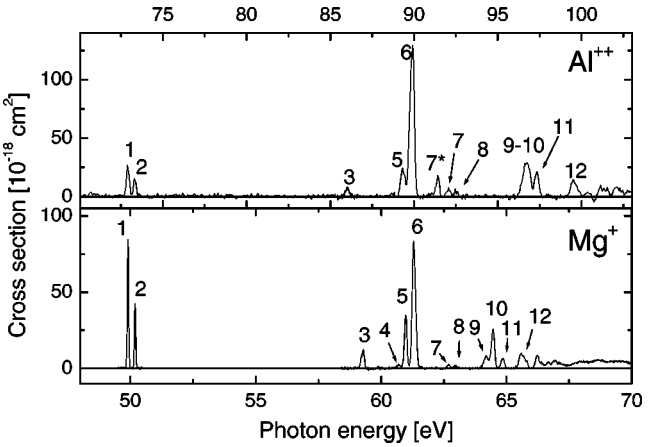

FIG. 6. Comparison between the photoionization spectra for Mg^+ [6] and Al^{2+} in the energy regions for excitation of a $2p$ electron.

we attribute to excitation of the metastable component. We propose that these structures are associated with excitation of the metastable $3s3p^3P$ state of Al^+, and in fact belong to the higher members of a $2p^5 3s3pnd$ series converging to the $2p^5 3s3p$ ionization limit at 98.3 eV. The energies of these levels would have to exceed the $2p^5 3s^2\,{}^2P_{3/2,1/2}$ thresholds at 91.71 eV or 92.16 eV, respectively, in order to autoionize into an excited state of Al^{2+}, which would then decay by an Auger transition to yield Al^{3+}. It should be noted that the metastable $3s3p\ {}^3P$ state is located 4.63 eV above the ground state; thus the structures observed in the double ionization channel above 88 eV are located energetically above these thresholds, if they originate from the metastable component. We have carried out calculations to determine the energies of the proposed nd levels and obtained energy values supporting the assignment of the dominant structures around 88.9 and 90 eV to $n=5$, 6, and 7. The complexity of the calculations does not allow us unambiguously to determine the dominant eigenvectors.

The assignment of the structure seen in the region above 92 eV (Fig. 1) has proved to be difficult. Here two window resonances, located at 93 eV and 96 eV, respectively, are observed in the double-ionization channel; these resonances were also observed in Ref. [8], but not identified. The photon energy excludes transitions from the $3s^2$ ground-state component, whereas excitation from either the $3p^2$ or metastable components may be possible. In case of the latter it is, however, necessary to assume two-electron excitation, which may be doubtful. It is not possible to identify these window-resonances unambiguously, but our calculations indicate that they are due to transitions from the $2p^6 3p^2\ {}^1S$ component of the ground state to the $2p^5 3p^2({}^1D)3d\ {}^1P$ and $4s\ {}^1P$ states.

The high-energy region of our spectra (Fig. 1) contains a prominent line at 122 eV followed by a weaker line at 132 eV. The analysis of these is relatively straightforward, recalling that in the corresponding region for Mg^+ members of the $2s \rightarrow np$ series could be identified, converging to a limit at 107.5 eV, close to the value expected theoretically. To our knowledge there are no corresponding experimental or theoretical data for the $2s$ ionization potential for Al^+, but the energy of the L_{I} edge for neutral aluminum is 117.7 eV, measured using electron spectroscopy on a solid sample [27]. We would therefore expect the value for Al^+ to be somewhat higher than this, so the strong line at 122 eV can be identified as the first member of the $2s \rightarrow np$ series, with $n=3$; the $n=4$ member is the line just discernible at 132 eV. A simple Rydberg analysis puts the series limit at 138(1) eV, in agreement with our Hartree-Fock calculated value of 139 eV.

B. Al^{2+}

The photoexcitation and ionization of the Al^{2+} ion have been studied over a limited photon-energy range, focusing on the resonance structures created by excitation of a $2p$ electron. Figure 6 shows the experimental data for Al^{2+} together with the data for the isoelectronic Mg^+ ion, which recently was the subject of a study in our laboratory [6]. There are clear similarities with the Mg^+ spectrum, and the results are to be compared not only with our Mg^+ measurements, but also with the dual-laser plasma measurements, assignments of Brilly *et al.* [11], and the MCHF calculations performed in connection with the present study.

The absolute continuum cross section is rather small, ~ 0.4 Mb over most of the energy region studied and dominated by photoionization of a $3s$ electron, but above 105 eV the cross section increases due to the opening of the $2p$ ionization channel. Above 105 eV the cross section reaches a value of ~ 6 Mb, in good agreement with the prediction by Combet Farnoux and Lamoureux [23]. The main effects of increasing the nuclear charge, in going from the Mg^+ to the Al^{2+} system, are that the $3s3d$ states appear at lower photon energies than the $3s4s$ states, whereas this order was reversed for Mg^+, and the spectrum is spread out over a larger energy range. The oscillator strengths for the $2p \rightarrow nd$ excitations are also increased considerably (Table III), indicating a much stronger transition moment between the wave functions involved for Al^{2+} than for Mg^+. Furthermore, the configuration interaction between the $3p^2\ {}^1D$ and $3s3d\ {}^1\mathrm{D}$ states is less prominent in the Al^{2+} ion, owing to the in-

TABLE III. The energies, identities, effective quantum numbers, and oscillator strengths (f values) for the $2p$ lines observed in Al^{2+}. The $1s^2 2s^2 2p^5$ part is omitted from the configurations.

Line No.	Energy (expt.) (eV)	Identity	n^*	Oscillator strength Expt.	Calculated
1	72.91	$(3s^2\ ^1S)^2P_{3/2}$	1.94	0.047	0.064
2	73.33	$(3s^2\ ^1S)^2P_{1/2}$	1.95	0.028	0.032
3a	85.94	$[(3p^2\ ^1D+3s3d\ ^1D)^2P_{1/2}]$	2.51	0.007	0.013
3b	86.07	$[(3p^2\ ^1D+3s3d\ ^1D)^2P_{3/2}]$	2.52	0.010	0.024
4		Not observed			
5	89.34	$(3s3d\ ^3D)^4D$	2.76	0.068	0.036
6	89.89	$(3s3d\ ^3D)^2P,\ ^2D$	2.81	0.377	0.377
7*	91.41	$(3s4s^3S)^2P$	2.96	0.043	0.029
7	92.06	$(3p^2\ ^1S)^2P_{3/2}$	3.03	0.019	0.015
8	92.52	$(3p^2\ ^1S)^2P_{1/2}$	3.08	0.014	
9	96.56	$(3s\ ^3P_{0,1,2})4d[5/2,3/2]$	3.72	0.061	0.260
10	96.83		3.78	0.078	
11	97.33		3.89	0.064	
12	99.55	$(3s^3P_{0,1,2})5d[5/2,3/2]$	4.58	0.061	
series limit	105.4 ± 0.3[a]				

[a]The series limit for the $2p^{-1}$ series was estimated by fitting Rydberg series to the $3d$, $4d$, and $5d$ lines and to the $3s$ and $4s$ lines, respectively.

creased influence of the nuclear charge. This may explain why less of the oscillator strength contained in the $2p \rightarrow nd$ transitions moves elsewhere in the spectrum, in comparison with the case for Mg^+.

The lines appearing at 72.91 eV and 73.33 eV (lines 1 and 2) can be assigned to the $2p^5 3s^2$ doublet P term, exhibiting an intensity ratio close to two as also observed for Mg^+. The following peaks at 85.94 eV and 86.07 eV can, with analogy to the Mg^+ study, be attributed to the doublet P state of the $(3p^2+3s3d)^1D$ complex with the dominant eigenvector being attributed to $3p^2$. The most intense feature in the Al^{2+} spectrum is, as also observed for Mg^+, line 6 that has a weaker structure, line 5, on its low-energy side.

On the basis of the theoretical calculations by Ivanov *et al.* [28] for photoabsorption and photoionization of the Mg^+ ion it was argued by Kjeldsen *et al.* [6] that line 6 in the Mg^+ spectrum ought to include the $3s3d\ ^1D$ term as the dominant eigenvector and consequently peak 6 should be assigned to the upper ^2P component of the $(3s3d + 3p^2)\ ^1D$ complex, whereas peak 5 could be accounted for by the doublet P component from the $2p^5 3s3d\ ^3D$ excitation. In addition, due to insufficient resolution it could not be excluded that the excitation of the $2p^5 3s4s\ ^3S$ component also contributed to peak 5. The calculations performed in connection with the present study have also included calculations of the resonance structures in the Mg^+ ion. Because configuration interaction is included by definition in the MCHF calculation it is considered more reliable than the random phase approximation with exchange (RPAE) calculations [28]; the RPAE method is in effect a one-electron calculation and is better suited to calculations of interactions between the continua of different ionization channels. It is therefore necessary to reassign the peaks 5 and 6 in the Mg^+ spectrum. Although they are still associated with the $3s3d$ configuration, our calculations indicate that they originate from the $2p^5(3s3d\ ^3D)^2P$ component, rather than the $2p^5(3s3d\ ^1D)^2P$ component originally proposed. Peak 5 can be attributed to the ^4D term, with an admixture from $(3s4s\ ^3S)^2P$, while the intense peak 6 should be assigned to a mixture of resonances originating from the $2p^5(3s3d\ ^3D)^2P$ and ^2D terms. Due to configuration interaction the strength of the $3s3d\ ^1D$ component is spread out over many, but weaker, resonance components. Therefore none of the observed structures can be assigned with $3s3d\ ^1D$ as the dominant eigenvector. See Table IV.

For the Al^{2+} ion the intensity ratio between peak 5 and peak 6 is smaller than observed for Mg^+. This observation can be accounted for by the displacement of the $3s4s$ configuration relative to the $3s3d$ configuration. The $2p^5(3s4s\ ^3S)^2P$ component will no longer contribute to peak 5, but will appear as a separate structure and has been identified as peak 7* in the Al^{2+} spectrum. Peak 6 will have the revised origin we have proposed above for the Mg^+ ion; peaks 7 and 8, tentatively identified as the doublet $3p^2\ ^1S\ ^2P_{3/2,1/2}$ in Mg^+, could be identified similarly in Al^{2+}, but Brilly *et al.* place these peaks at an energy just below peak 7* rather than above it so their identity must remain uncertain. Table III contains the assignments of all the structures observed in Al^{2+} in Fig. 6 together with the effective quantum numbers, the measured, and the calculated oscillator strengths. Our CI calculation yielded oscillator strengths for 46 levels belonging to 27 terms that we have used to help us to make assignments. The present assignments are generally in good agreement with those put forward by Brilly *et al.* [11]. The agreement among the experimental observations, the associated calculations for the present study, and the laser plasma study by Brilly *et al* gives confidence in these assign-

TABLE IV. The energies, identities, and oscillator strengths (f values) for the $2p$ lines observed in Mg^+. The $1s^2 2s^2 2p^5$ part is omitted from the configurations.

Line No.	Energy (expt. [a]) (eV)	Identity	Oscillator strength Expt. [a]	Calculated
1	49.90	$(3s^2\ ^1S)^2P_{3/2}$	0.049	0.054
2	50.18	$(3s^2\ ^1S)^2P_{1/2}$	0.025	0.027
3a	59.21	$(3p^2\ ^1D+3s3d\ ^1D)^2P_{1/2}$	0.006	0.005
3b	59.30	$(3p^2\ ^1D+3s3d\ ^1D)^2P_{3/2}$	0.010	0.009
4	60.71	$(3p^2\ ^3P)^2P$	0.002	
5	60.98	$(3s3d\ ^3D)^4D$, $(3s4s\ ^3S)^2P$	0.040	0.037
6	61.34	$(3s3d\ ^3D)^2P$, ^2D	0.122	0.134
7	62.71	$(3p^2\ ^1S+3s^2\ ^1S)^2P_{3/2}$	0.003	
8	63.00	$(3p^2\ ^1S+3s^2\ ^1S)^2P_{1/2}$	0.002	
9	64.19	$3s\ ^3P_2 4d_{3/2}$, $3s\ ^3P_2 5s_{1/2}$, $3s\ ^3P_1 4d_{3/2,5/2}$	0.013	0.007
10	64.48	$3s\ ^3P_1 5s_{1/2}$, $3s\ ^3P_0 4d_{3/2}$, $3s\ ^3P_0 5s_{1/2}$, $3s\ ^3P_2 4d_{5/2}$	0.039	0.022
11	64.90	$3s\ ^1P_1 5s_{1/2}$, $3s\ ^1P_1 4d_{3/2,5/2}$,	0.010	0.006
12	65.61	Sum of (3s6s) and (3s5d) lines	0.026	

[a]From Kjeldsen *et al.* [6].

ments. In Table IV we give the new assignments of the Mg^+ resonances seen in Fig. 6 together with the previously measured [6] and the new calculated oscillator strengths. A comparison between Tables III and IV illustrates the effect of the increased nuclear charge changing from Mg^+ to Al^{2+}. Whereas the oscillator strengths are nearly the same for $2p$ excitation to the ns series, the oscillator strengths for the nd series are much larger for the Al^{2+} ion, as seen both from the experimental data and from the calculated values.

V. CONCLUSION

The present measurements of the absolute photoionization cross sections for Al^+ and Al^{2+} ions show that the previously published calculated continuum cross sections for these ions are reliable and can be used for modeling of astrophysical and other plasmas. The resonance structure investigations have shown good agreement between the present data and structures observed from laser-produced plasmas, but additional structures have been observed such as a series of window resonances of the type $2p^6 3pns$ belonging to the Al^+ ion together with a collection of structures related to core excitation of the $2p^6 3s3p$ or $3p^2$ configurations. Further studies are needed to give unambiguous assignments for the latter. The Al^{2+} spectra exhibit many of the same resonances also observed for Mg^+, but the oscillator strengths for the $2p \rightarrow nd$ transitions are much larger for Al^{2+} than for Mg^+. The comparison between the synchrotron radiation spectra of the isoelectronic Mg^+ and Al^{2+} ions have resulted in a revision of the recent assignment of the dominant resonance structure belonging to Mg^+. This revision indicates that advanced calculations are needed for support of assignments where configuration interactions dominate the spectra.

ACKNOWLEDGMENTS

The ion-photon project is part of the research program for the Aarhus Center for Atomic Physics (ACAP), funded by the Danish National Research Foundation. We are grateful to the staff of the Institute for Storage Ring Facilities (ISA) at University of Aarhus for their expert assistance throughout the period of the project. We thank Tomas Brage for help with the calculations. One of us (R.L.B.) would like to thank the Aarhus Center for Atomic Physics for support during his research sabbatical.

[1] *The Opacity Project* (Institute of Physics, Bristol, UK, 1995), Vol. 1.
[2] F. J. Rogers and C. A. Iglesias, Science **263**, 50 (1994).
[3] S. N. Nahar and A. K. Pradhan, Phys. Rev. A **49**, 181 (1994).
[4] I. C. Lyon, B. Peart, J. B. West, and K. Dolder, J. Phys. B **19**, 4137 (1986).
[5] H. Kjeldsen, F. Folkmann, J. E. Hansen, H. Knudsen, M. S. Rasmussen, J. B. West, and T. Andersen, Astrophys. J. **524**, L143 (1999).
[6] H. Kjeldsen, J. B. West, F. Folkmann, H. Knudsen, and T. Andersen, J. Phys. B **33**, 1403 (2000).
[7] J-M. Esteva and G. Mehlman, Astrophys. J. **193**, 747 (1974).
[8] J. T. Costello, D. Evans, R. B. Hopkins, E. T. Kennedy, L. Kiernan, M. W. D. Mansfield, J-P. Mosnier, M. H. Sayyad, and B. F. Sonntag, J. Phys. B **25**, 5055 (1992).
[9] J-P. Mosnier, J. T. Costello, E. T. Kennedy, L. Kiernan, and

M. H. Sayyad, Phys. Rev. A **49**, 755 (1994).
[10] W. C. Martin and R. Zalubas, J. Phys. Chem. Ref. Data **8**, 826 (1979).
[11] J. Brilly, E. T. Kennedy, and J-P. Mosnier, J. Phys. B **21**, 3685 (1988).
[12] J. W. G. Thomason and B. Peart, J. Phys. B **31**, L201 (1998).
[13] H. Teng, J. Phys. B **33**, L553 (2000).
[14] U. V. Becker and D. A. Shirley, *VUV and Soft X-Ray Photoionization* (Plenum Press, New York, 1996).
[15] V. Schmidt, *Electron Spectroscopy of Atoms Using Synchrotron Radiation* (Cambridge University Press, Cambridge, England, 1997).
[16] H. Kjeldsen, F. Folkmann, H. Knudsen, M. S. Rasmussen, J. B. West, and T. Andersen, J. Phys. B **32**, 4457 (1999).
[17] M. Domke, K. Schulz, G. Remmers, G. Kaindl, and D. Wintgen, Phys. Rev. A **53**, 1424 (1996).
[18] D. A. Shaw, G. C. King, and F. H. Read, Chem. Phys. Lett. **129**, 17 (1986).
[19] O. Almen and K. Nielsen, Nucl. Instrum. Methods **1**, 302 (1957).
[20] C. Froese Fischer, T. Brage, and P. Jönsson, *Computational Atomic Structure: An MCHF Approach* (Institute of Physics, Bristol, 1997).
[21] T. Andersen, T. Brage, C. Froese Fischer, and L. Eg Sorensen, J. Phys. B **24**, 905 (1991).
[22] C. Froese Fischer and B. Liu, Comput. Phys. Commun. **64**, 406 (1991).
[23] F. Combet Farnoux and M. Lamoureux, J. Phys. B **9**, 897 (1976).
[24] P. C. Deshmukh, G. Nasreen, and S. T. Manson, Phys. Rev. A **38**, 504 (1988).
[25] K. Butler, C. Mendoza, and C. J. Zeippen, J. Phys. B **26**, 4409 (1993).
[26] J. B. West, K. Codling, and G. V. Marr, J. Phys. E **7**, 137 (1974).
[27] R. Nordberg, K. Hamrin, A. Fahlman, C. Nordling, and K. Siegbahn, Z. Phys. **192**, 462 (1966).
[28] V. K. Ivanov, J. B. West, G. F. Gribakin, and A. A. Gribakina, Z. Phys. D: At., Mol. Clusters **29**, 109 (1994).